Detailed experimental and numerical characterization of turbulent flow in components of a water treatment plant

Ivan Matías Ragessi, Carlos Marcelo García, Santiago Márquez Damián, Cecilia Pozzi Piacenza and Mariano Ignacio Cantero

ABSTRACT

This paper presents a detailed characterization of turbulence in the incoming flow to the clarification component of a water treatment plant, 'Los Molinos' (Córdoba, Argentina). The main problems were related to the presence of turbulent flow patterns throughout the treatment, affecting the proper development of the physical processes required for water clarification. Namely: (a) a poor hydraulic design that could produce a non-homogeneous spatial distribution of the flow, recirculation zones and flow stagnation, and a non-uniform discharge distribution among the sedimentation units as a result of different cross-sectional dimensions of the transverse-channel, and (b) high turbulence intensity that affect the flocs' size as well as the efficiency of the settling tanks and filters. Firstly, a detailed in-situ experimental characterization of the turbulent flow was undertaken. An acoustic Doppler velocimeter (ADV) was used to characterize the flow turbulence, whereas for discharge measurements and mean flow velocity field an acoustic Doppler current profiler (ADCP) was employed. Secondly, a numerical model, based on the Reynolds-averaged Navier–Stokes (RANS) equations and the k-ϵ turbulence closure model, was validated with the experimental data. Finally, based on the results, a diagnosis and recommendations were made for the optimization of the hydraulic design of the water treatment plant.

Key words | acoustic Doppler velocimetry, CFD, clarification process

Ivan Matías Ragessi (corresponding author)
Cecilia Pozzi Piacenza
Centro de Estudios y Tecnología del Agua (CETA).
Laboratorio de Hidráulica (LH). Facultad de Ciencias Exactas, Físicas y Naturales,
Universidad Nacional de Córdoba.
Av. Velez Sarsfield 1611, Ciudad Universitaria,
Córdoba,
Argentina
E-mail: *matiasragessi@gmail.com*

Carlos Marcelo García
Instituto de Estudios Avanzados en Ingeniería y Tecnología (IDIT CONICET/UNC) y CETA.
Facultad de Ciencias Exactas, Físicas y Naturales – Universidad Nacional de Córdoba,
Av. Velez Sarsfield 1611, Ciudad Universitaria,
Córdoba,
Argentina

Santiago Márquez Damián
Centro de Investigación de Métodos Computacionales (CIMEC), UNL/CONICET,
Colectora Ruta Nac. 168. Paraje El Pozo (300)
Santa Fe,
Argentina

Mariano Ignacio Cantero
Consejo Nacional de Investigaciones Científicas y Técnicas (CONICET), División de Mecánica Computacional, Centro Atómico Bariloche,
Comisión Nacional de Energía Atómica (CNEA)/ Instituto Balseiro (IB – CNEA – UNC),
Bariloche,
Argentina

INTRODUCTION

The optimization of existing drinking water treatment plants has an important significance in satisfying the increasing needs for drinking water of a growing population in large urban agglomerations. The design and evaluation of this type of infrastructure is usually done according to sanitary engineering criteria (Adams *et al.* 1999). However, hydrodynamic singularities of the flow during the water treatment process can greatly affect their performance due to the incompatible high turbulence flow intensity with respect to the intended sanitarian design.

On the one hand, turbulence is considered as a determining factor in a variety of problems in engineering, for instance the coagulation-flocculation step. It is well known that the floc size is directly related to the Kolmogorov scale and, thus, to the dissipation rate of turbulent kinetic energy. On the other hand, the coagulation-flocculation step is a relevant process in drinking water treatment plants and is used in 95% of such facilities. Therefore, it is important to optimize both the coagulant dosification as well as the hydraulic design in order to minimize the turbulence intensity (and, therefore, avoid floc break) throughout this part of the treatment.

In this context, there is a need to characterize in detail the turbulent flow in the different hydraulic components of water treatment plants in order to evaluate some incompatible tri-dimensional flow patterns with respect to the physical

doi: 10.2166/wst.2020.013

conditions required in the treatment process (e.g. mixing, flocculation and sedimentation).

This paper reports a detailed experimental and numerical characterization of the incoming turbulent flow into the clarification process of the water treatment plant 'Los Molinos' (Figure 1) operated by the Aguas Cordobesas SA Company in Bower, near the capital city of Cordoba province, Argentina (from now on, the water treatment plant).

This water treatment plant supplies drinking water to approximately 30% of the population of the city of Córdoba and together with the Suquia water treatment plant supplies drinking water to approximately 1.4 million people.

The main problems observed in the study case are related to the presence of turbulent flow patterns throughout the treatment process that could affect the proper development of the physical conditions required for water clarification. Namely:

(a) a poor hydraulic design that could produce a non-homogeneous spatial distribution of the flow, recirculation zones and flow stagnation, and a non-uniform discharge distribution among the sedimentation units as a result of different dimensions of the cross-sections in the transverse-channel (see Figure 1); and
(b) high turbulence intensity that could affect the floc's size and the efficiency of the clarifiers and filters.

In order to evaluate the effects of the above mentioned problems on the treatment plant efficiency, a detailed spatial and temporal characterization of the incoming turbulent flow into the clarification component was made for different operational conditions. This characterization has been done by experimental measurements and numerical modeling.

Firstly, the experimental characterization was made with two advanced flow velocity measurement techniques: (a) an acoustic Doppler velocimeter (ADV) that samples high-temporal resolution time series of the three velocity vector components; and (b) an acoustic Doppler current profiler (ADCP) that records vertical profiles of the three velocity vector components.

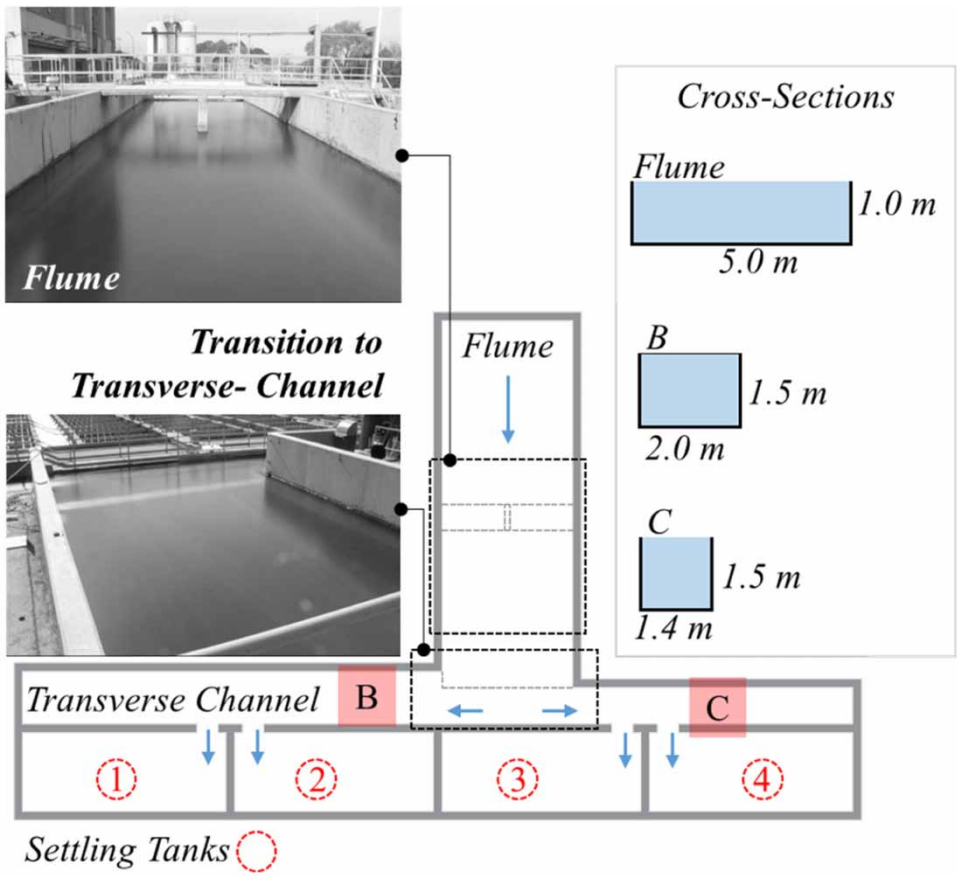

Figure 1 | Plain view of the flume, transverse-channel and cross-sections dimensions. The flume and transverse-channel length is 29 meters and 23.3 meters, respectively. Water treatment plant 'Los Molinos'. The arrows indicate the flow direction.

Secondly, a numerical model, based on the Reynolds-averaged Navier–Stokes (RANS) equations and the k-ϵ turbulence closure model, was validated with experimental data: comparing mean velocity fields, size and location of the recirculation and stagnation zones, three-dimensional flow structures, values of turbulent kinetic energy (k), dissipation rate (ϵ), and inflow discharge to each clarification unit. In this study OpenFOAM® (OpenCFD), an open-source toolbox, was used.

There are recent technological and scientific advances dedicated to optimize water treatment processes using in-situ experimental techniques, and so the use of ADV and ADCP techniques begins to be relevant. Garcia & Garcia (2006) have characterized the flow turbulence and the mixing induced by air-bubble plumes in wastewater reservoirs in non-stratified conditions using ADV measurements. Kiss & Patziger (2013) used ADV for a better understanding of flow patterns in a primary sedimentation tank of a wastewater treatment plant. Also, ADCP has been used to characterize the flow in clarifiers describing the key physical processes: hydrodynamics, particle aggregation and floc breaking (De Clercq *et al.* 2002; Vanrolleghem *et al.* 2006).

Numerical models have also been an important alternative for studying turbulent flows on hydraulic components of water and wastewater treatment plants (Huggins *et al.* 2004; Goula *et al.* 2008; Shahrokhi *et al.* 2011; Zhang 2014). Most of these works remark the importance of dissipating as much energy as possible in the incoming flow in order to improve the settling tanks' efficiency. So, the design of the incoming flow structures is of great importance, not only to avoid incompatible values of turbulent kinetic energy in the tank, but also to avoid floc breaks and to ensure the settling efficiency of tanks and filters. Also, research has been done about the size and position of baffles and their effects on the inlet flow, in order to minimize recirculation zones and improve the floc removal efficiency (Huggins *et al.* 2004; Goula *et al.* 2008; Zhang 2014). The main objective was to establish specific criteria and provide design guidelines for engineers.

More recently, Patziger & Kiss (2015) have calibrated and validated a primary settling tank tridimensional model, based on experimental in-situ measurements (ADV and optical turbidity meter) and settling tests.

Also, Patziger *et al.* (2016) reported the results of a comprehensive investigation programme on the design and operation of primary settling tanks for wastewater treatment. Removal efficiency, settling properties of primary sludge, internal flow structures within primary settling tanks and the impact on their performance were investigated and evaluated. According to Wei *et al.* (2016), the flow fields of a pilot Carrousel oxidation ditch can be accurately simulated by LES (large eddy simulation) with the Smagorinsky model, based on experimental validation. They established how to calculate the best submerged depth value in the surface aerators in order to improve the pollutant removal capability and to prevent sludge deposition.

On the other hand, Samstag *et al.* (2016) provide an overview of CFD (computational fluid dynamics) applied to a wide different range of unit processes in water and wastewater treatment plants. They articulate the state of practice, research and development needs. In addition, they conclude that CFD is nowhere used (except possibly in the disinfection process) as a routine tool for design, risk-management, or troubleshooting. Laurent *et al.* (2014) presented a protocol to develop more practical and everyday use of CFD models.

Finally, Wicklein *et al.* (2016) tried to briefly outline the principal features of good modeling practice for wastewater treatment as part of the International Water Association (IWA) investigation work. The main objective was to guide new modelers in the application of CFD studies in the wastewater field.

The aforementioned study indicates that the flow turbulence characterization in water treatment plant components is still a challenge and that it is of great convenience to complement modern experimental techniques with numerical tools in order to obtain a more detailed flow characterization.

It must be emphasized that the validation of the CFD model is crucial. Firstly, CFD can be used for optimizing the hydraulic design and to improve the effluent quality. Secondly, it could increase the basic understanding of internal processes and their interactions. This knowledge can, again, be used for process optimization.

Finally, based on the experimental data and the results of numerical modeling, a diagnosis and several recommendations were made for the optimization of the hydraulic design and the operation of the plant. This validated model is now available as a tool for Aguas Cordobesas SA to apply it to future studies in order to optimize the hydraulic design of the components.

MATERIALS AND METHODS

Six in-situ measurements were performed in order to experimentally characterize the incoming flow to the clarification

units, representing six different plant operating conditions; that is, flow discharges between 1.33 m^3/s and 2.10 m^3/s, according to the acoustic flowmeter installed in the plant. The latter value is above the design water treatment plant capacity, and was due to the strong seasonal variations in drinking water consumption in Cordoba city. The main characteristics of the tested experimental conditions (including the number of operating settling tanks) are reported in Table 1. All the in-situ measurements at the treatment plant are ordered chronologically.

The turbulent flow in the study area presents large spatial and temporal variations. The characteristic spatial and temporal scales of the largest turbulent structures are estimated about 1 meter and 1 second respectively based on the mean flow velocity values (about 1 m/s) and geometry of the channel (water depth about 1 m), while the smaller spatial scales are expected to be around 0.0001 meter (validated later in this paper). So, the experimental work not only requires measurement techniques that can be applied to large experimental facilities, but also for them to be capable of sampling high spatial and temporal variations in order to obtain relievable flow turbulent parameters (mean velocities, turbulent fluctuations, characteristic scales of the problem, etc.).

Some preliminary tests indicated that the concentration of suspended particles in the flow was appropriate for the use of both acoustic Doppler techniques (García & Herrero 2009). The main characteristics of the experimental techniques implemented in this work are summarized in the following subsections.

Acoustic Doppler velocimetry (ADV)

A MicroADV Sontek® 16 MHz was used, recording time series of the velocity vector components within a measurement volume of 4.5 mm in diameter and 5.6 mm of height and using recording frequencies of up to 50 Hz. During in-situ measurements 1 and 2, specific experimental methods developed by García & Herrero (2009) were applied. Time series were recorded in ten locations in section A-A (Figure 2(a)): five points at 0.25 m and 0.75 m from the flume bottom, and separated horizontally 1 m from each other. In sections B-B and C-C (see Figure 2(a)), sampling was made at four vertical locations across sections' width at three depths from the free surface: 0.07 m, 0.27 m; and 0.67 m. Sections B-B and C-C are located at X-axis 15.25 m; y 21.85 m, respectively. Finally, at locations D and E, flow velocity measurements were performed in the center line (X-axis 22.9 m and 24.7 m in Figure 2(a)) at 0.15 m upstream of each gate, at 0.88 m, 1.28 m and 1.48 m from the transverse-channel bottom. In each section and gates' flow discharges, three-dimensional flow patterns and turbulence intensity were quantified.

Table 1 | Experimental conditions evaluated in each filed work

In-situ measurements	Date	Number of settling tanks in operation	Flow depth [m]	Flow discharge measured by the plant acoustic-flowmeter [m^3/s]
1	06/10/2009	3	0.94	1.53
2	07/09/2009	4	0.94	1.55
3	09/23/2010	4	0.95	1.33
4	07/05/2009	4	0.94	1.67
5	02/15/2011	4	0.94	1.67
6	07/08/2011	4	0.94	1.87
7	12/27/2011	4	0.99	2.10

Acoustic Doppler current profiler (ADCP)

This acoustic technique provides commonly three-dimensional mean flow velocity information and is used worldwide to characterize turbulent flows in river systems and artificial channels. The ADCP used in this study is a RiverSurveyor S5 YSI/Sontek.

Based on flow depth and mean flow velocity, this ADCP adapts the acoustic pulse scheme in order to obtain high spatial data resolution (with cells up to 2 cm) at 1 Hz frequency. In the in-situ measurements, 3, 4, 5, 6 and 7 vertical velocity profiles were recorded in different locations (see Figure 2(b)): (1) Section F-F (flume cross-section at Y-axis 9.0 m) for discharge measurements, Section G-G (longitudinal section at flume centerline at X-axis 18.55 m), and Section H-H (longitudinal profile at the centerline of the transverse-channel). These measurements provide the mean flow velocity fields (i.e. secondary flows, recirculation zones, etc.). Finally, the inlet flow discharges for each sedimentation tank were quantified using measurements at the center line of the gates 1, 2, 3 and 4 (at X-axis 7.1 m, 8.85 m, 22.9 m and 24.7 m, respectively).

NUMERICAL MODELING OF TURBULENT FLOW

Reynolds-averaged Navier-Stokes (RANS) equations with a k-ϵ standard turbulence closure model (Launder & Sharma 1974) was used to simulate three-dimensional flow in the study area and to detect recirculation and high turbulence intensity zones.

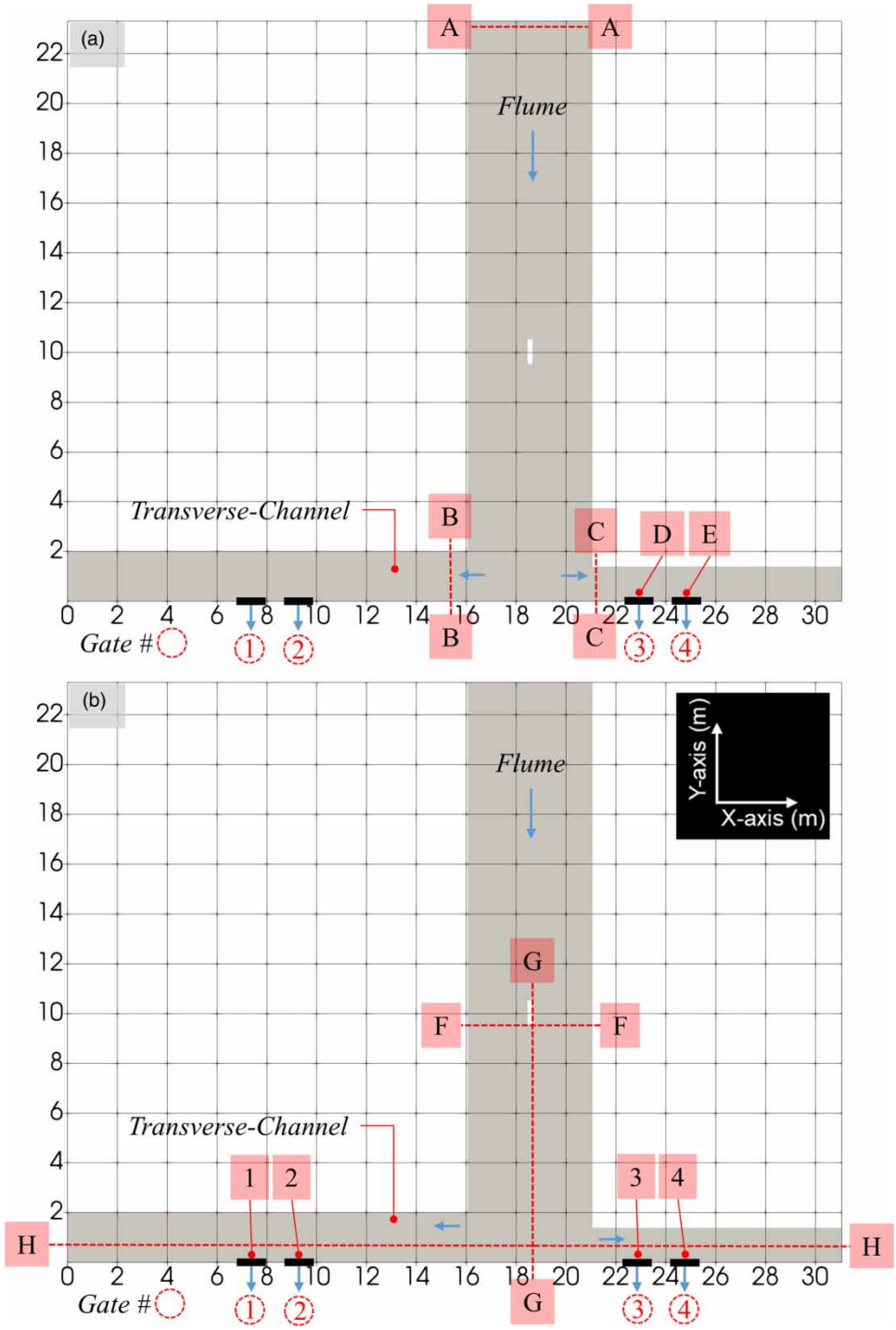

Figure 2 | Scheme of the studied area and location of the measuring sections with ADV (a) and ADCP (b). The blue arrows indicate the flow direction. Please refer to the online version of this paper to see this figure in color: http://dx.doi.org/10.2166/wst.2020.013.

The 'Semi-Implicit Method for Pressure-Linked Equations' scheme (simpleFoam in OpenFOAM®) has been used to solve the Navier-Stokes equations with an iterative process using the finite volume method. The simpleFoam scheme applies to single phase steady flow, with constant density and viscosity (Versteeg & Malalasekera 2007; OpenFOAM Wiki. The SIMPLE algorithm in OpenFOAM).

RANS equations model considering steady-state, incompressible flow and a standard k-ϵ closure model is presented in Equations (1)–(5). Equation (1) is the continuity equation for incompressible flow; Equation (2) is the RANS equations considering the Boussinesq approximation. This approximation adds a new unknown to the system: μ_T (turbulent viscosity), which is estimated using Equation (3). Finally, Equations (4) and (5) are the transport equations for k and ε required to determine the value of μ_T in the selected turbulent closure model.

$$\frac{\partial \bar{u}_i}{\partial x_i} = 0 \tag{1}$$

$$\rho\left(\bar{u}_i \frac{\partial \bar{u}_i}{\partial x_j}\right) = -\frac{\partial \bar{p}}{\partial x_i} + \frac{\partial}{\partial x_j}\left[\mu\left(\frac{\partial \bar{u}_i}{\partial x_j} + \frac{\partial \bar{u}_j}{\partial x_i}\right)\right] + \frac{\partial}{\partial x_j}\left[\mu_T\left(\frac{\partial \bar{u}_i}{\partial x_j} + \frac{\partial \bar{u}_j}{\partial x_i}\right)\right] + \frac{\partial}{\partial x_j}\left[\frac{2}{3}\rho k \delta_{ij}\right] \tag{2}$$

$$\mu_T = \rho C_\mu \frac{k^2}{\epsilon} \tag{3}$$

$$\left(\bar{u}_j \frac{\partial k}{\partial x_j}\right) = \frac{\partial}{\partial x_j}\left[\frac{\mu_T}{\sigma_k}\left(\frac{\partial \bar{u}_i}{\partial x_j} + \frac{\partial \bar{u}_j}{\partial x_i}\right)\right] + \mu_T\left[\frac{\partial \bar{u}_i}{\partial x_j}\left(\frac{\partial \bar{u}_i}{\partial x_j} + \frac{\partial \bar{u}_j}{\partial x_i}\right)\right] - \rho\epsilon \tag{4}$$

$$\rho\left(\bar{u}_j \frac{\partial \epsilon}{\partial x_j}\right) = \frac{\partial}{\partial x_j}\left[\frac{\mu_T}{\sigma_\epsilon}\left(\frac{\partial \bar{u}_i}{\partial x_j} + \frac{\partial \bar{u}_j}{\partial x_i}\right)\right] + C_{1\epsilon}\frac{\epsilon}{k}\mu_T\left[\frac{\partial \bar{u}_i}{\partial x_j}\left(\frac{\partial \bar{u}_i}{\partial x_j} + \frac{\partial \bar{u}_j}{\partial x_i}\right)\right] - C_{2\epsilon}\rho\frac{\epsilon^2}{k} \tag{5}$$

Here: $\bar{u}_i$: the mean i component of velocity vector (i = 1–3), $\bar{p}$: mean pressure, ρ: water density, μ: momentum diffusivity (viscosity), k: turbulent kinetic energy, μ_T: turbulent viscosity, ϵ: rate of dissipation of k, δ_{ij}: Dirac delta function, σ_k: ratio of momentum diffusivity (viscosity) and k diffusivity, σ_ϵ: ratio of momentum diffusivity (viscosity) and ϵ diffusivity, C_μ,$C_{1\epsilon}$, $C_{2\epsilon}$ are k-ϵ model parameters. In this work, $\sigma_k = 1.00$, $\sigma_\epsilon = 1.30$, $C_\mu = 0.09$, $C_{1\epsilon} = 1.44$ and $C_{2\epsilon} = 1.92$ based on Launder & Spalding (1972, 1974) recommendations as implemented in OpenFOAM®. These parameters have not been modified in this work.

Computational domain

The spatial discretization of the computational domain (Figure 3(a)) has been performed with a mesh of variable volumes. A mesh convergence analysis was performed in order to select a mesh that offered acceptable results with a relatively low computational cost. Near the bottom and walls, volumes are 2.5 cm wide, increasing their width to 3.5 cm, 5 cm and 6 cm towards the center of the domain. The central domain zone contains volumes of equal size. The mesh was densified in the area where the flow has a transition from the flume to the transverse-channel (Figure 3(b)). The structured mesh is composed of 339,976 hexahedrons.

Boundary and initial conditions

Table 2 summarizes the boundary conditions imposed on the computational domain.

RESULTS

Validation of the numerical model

The validation of the numerical model was done comparing experimental data and numerical simulation results in sections B-B and C-C (transverse-channel in Figure 2(a)). The data collected in the flume (section A-A in Figure 2(a)) are not included in the validation because the experimental values were used as an inlet boundary condition in the numerical model. Also, to determine whether the observed differences between experimental and numerical results are statistically significant, confidence intervals of the experimental values were used. In this work, the Moving Block Bootstrap (MBB) technique, proposed by García *et al.* (2006), was used to estimate confidence intervals for different turbulent parameters.

Figure 4(a) and 4(b) compare the numerical model results with the experimental data (from in-situ measurements 2, see Table 1) in both sections, B-B and C-C (transverse-channel). The mean longitudinal-velocity values were similar for the three depths, respectively.

The larger differences are observed for the deepest locations in both sections (B-B and C-C). In these zones, a non-stationary phenomenon occurs that could explain the largest differences found. Figure 4(a) and 4(b) also show that there are large areas in cross-sections B-B and C-C that do not significantly contribute to the main flow and that recirculation affects 50% of the cross-section width. The secondary flow velocity and the streamflow indicate two counterclockwise recirculation cells in section B-B (Figure 4(c)) and two clockwise cells in section C-C (Figure 4(d)).

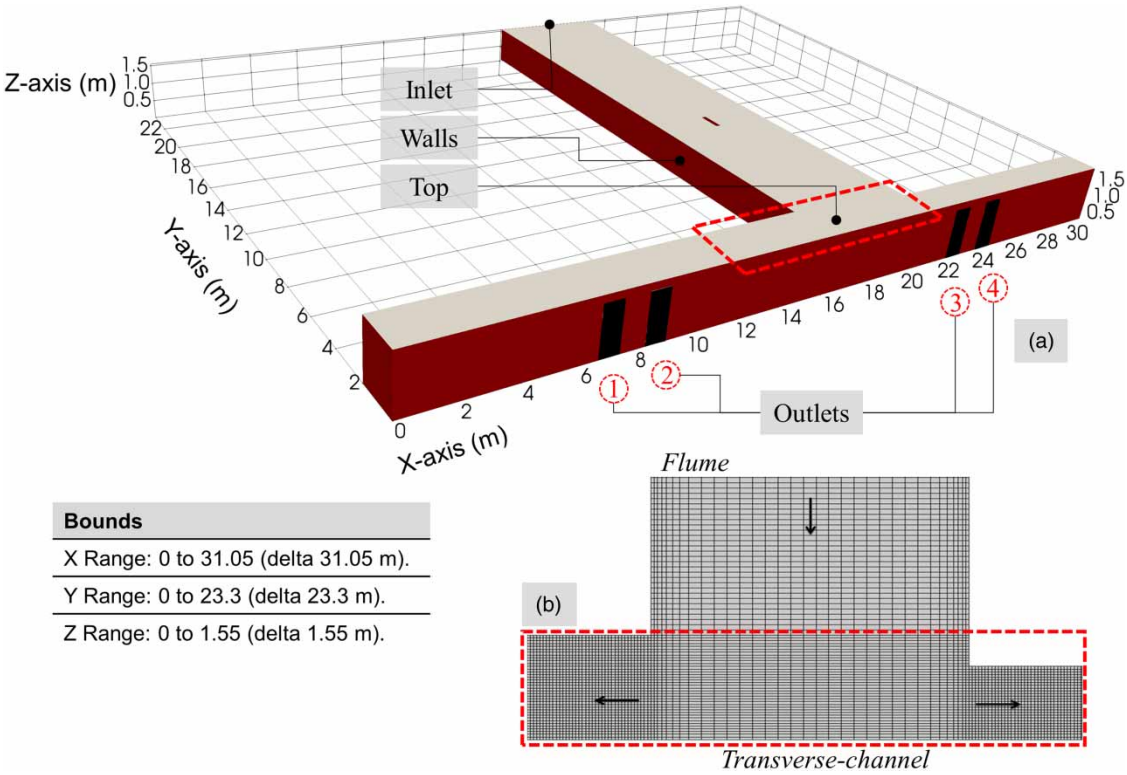

Figure 3 | (a) Computational domain and (b) the computational grid transition zone from the flume to the transverse-channel.

Table 2 | Boundary conditions adopted for RANS simulations

Region	$\bar{u}_i$	$\bar{p}$	k	ε
Inlet	Mean velocity values measured experimentally in cross-section A-A	$\vec{\nabla} p \cdot \vec{n} = 0$	Calculated from experimentally measured data in cross-section A-A	Estimated from experimentally measured data in cross-section A-A
Outlet	$\overrightarrow{\nabla \cdot} \vec{U} = 0$	Average static pressure at the faces of the volumes	$\vec{\nabla} k \cdot \vec{n} = 0$	$\vec{\nabla} \epsilon \cdot \vec{n} = 0$
Wall/bottom	0 (zero)	$\vec{\nabla} p \cdot \vec{n} = 0$	kqRWallFunction[a]	epsilonWallFunction[a]
Free surface	Slip	$\vec{\nabla} p \cdot \vec{n} = 0$	$\vec{\nabla} k \cdot \vec{n} = 0$	$\vec{\nabla} \epsilon \cdot \vec{n} = 0$

[a]kqRWallFunction and epsilonWallFunction are standard OpenFOAM® wall functions for k y ϵ used in wall and bed, see Takano & Moonen (2013) and Robertson *et al.* (2015).

Figure 5(a) and 5(b) show the results at locations close to gates 3 and 4 (points D and E, see Figure 2). The mean longitudinal flow velocity profile (incoming flow to each gate) resulting from the numerical model and the one recorded with the ADV are quite similar.

The mean inlet velocity at gate 3 is 50% smaller than at gate 4, so the inlet discharge at settling tank 4 is larger and thus has a smaller detention time All this results in a lower floc removal efficiency.

Table 3 summarizes the maximum values of k from the experimental data and the ones from the numerical model for flow conditions 2 (see Table 1). The experimental values k have been computed using the observed values of velocity variances $k = 0.5\ (u_i'2)^{1/2}$ while the numerical values have been computed using the standard k-ϵ model. The numerical data indicate the maximum value of each section.

This table also includes confident intervals estimated using the MBB method. Even though the experimental

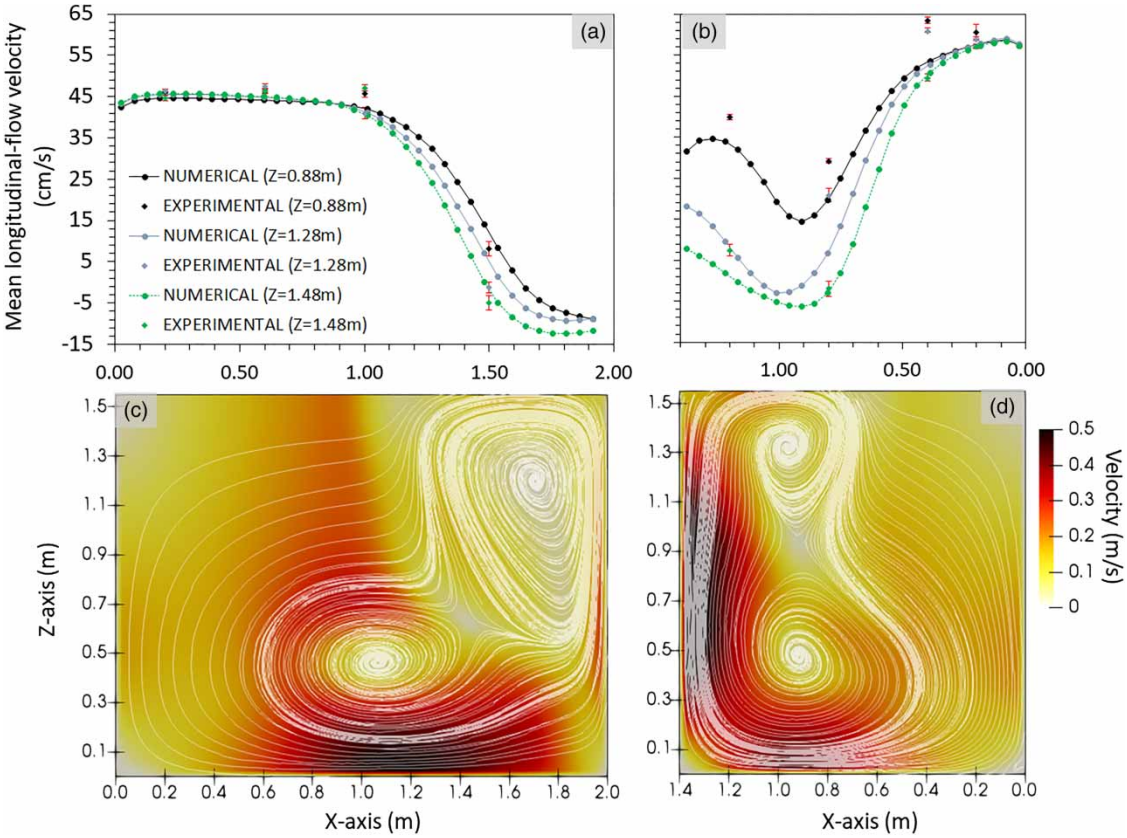

Figure 4 | Mean longitudinal flow velocity values comparing numerical model and experiment observations (in-situ measurement 2) for section B-B (a) and section C-C (b) at different distances from the bottom (Z). Secondary flow velocity for section B-B (c) and section C-C (d). In X-axis, 0 indicates the left bank of the transverse-channel in (a) and (c) and right bank in (b) and (d).

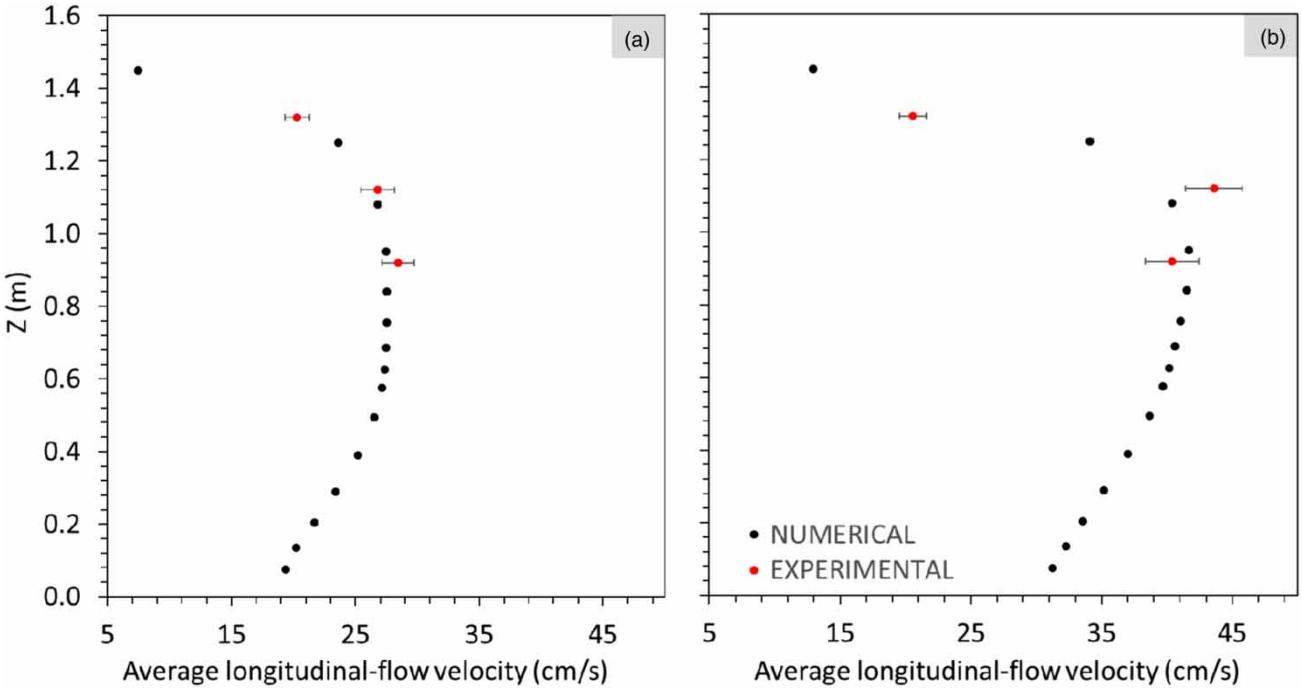

Figure 5 | Comparison of the values of the average longitudinal flow velocity resulting from numerical model and ADV measurements at location near gates 3(a) and 4(b) (points D and E in Figure 2(a)). Flow conditions present in the in-situ measurements 2.

Table 3 | Maximum values of turbulent kinetic energy k [cm^2/s^2] experimentally observed and numerically simulated in different cross-sections of the study area for flow conditions present in in-situ measurements 2

Section	Experimental k	Numerical k
Flume	50 ± 5	50[a]
Section B-B	128 ± 13	191
Section C-C	494 ± 44	554
Gate 3	369 ± 37	385
Gate 4	339 ± 51	447

[a]Boundary inlet flow condition.

Table 4 | Values of ϵ [cm^2/s^3] estimated and numerically simulated at various cross-sections of the plant for flow conditions present in in-situ measurements

Section	Experimental ϵ	Numerical simulation ϵ
Flume	2.19	7.7
Section B-B	42.66	115.3
Section C-C	414.54	310.85
Point D	162.42	212.4
Point E	20.68	119.3

and numerical values of k are statistically different in sections C-C and in gates 3 and 4, both sets of data show similar trends: k values near the gates and in section C-C are one order of magnitude larger than the values of k in the incoming flow (flume). This observation does not agree with standard sanitary design guidelines.

The observed differences in the k values in section C-C, gates 3 and 4, can be due to the outlet boundary condition used: an average static pressure at the faces of the volumes. This is not completely true, since flow changes over time imply changes in the total pressure values. It is important to mention that a k-Omega SST model was used for the same domain and no significant improvements were observed in the velocity distribution and absolute k values.

The high turbulence intensity in the mentioned locations may affect the floc size. Ducoste *et al.* (1997) claim that the maximum floc size, d_{max}, is related to the average intensity of the turbulent fluid motion. These authors presented a formula to estimate d_{max} as a function of ϵ, the turbulent dissipation rate of k. Their formula presents variations with respect to other formulas presented by different authors as:

$$d_{max} = C/\epsilon^n$$

where C is a coefficient related to the strength of the floc particles and n is a coefficient related to the breakup mode. This formula shows that the higher the value of ϵ, the smaller the expected maximum floc size d_{max}. Table 4 shows values of ϵ estimated at different locations both from experimental results and numerical simulations.

The values of ϵ from the experimental observations were estimated as $\epsilon = k^{2/3}/L$, where L is the scale of the largest eddies present in the flow. Scales L were estimated from the correlation analysis of temporal flow velocity signals at each location and Taylor's Frozen approximation (Garcia & Garcia 2006). The numerical values of ϵ have been computed using the standard k-ϵ model. Comparisons of the numerical and experimental values of ϵ show a very good agreement and therefore indicate the relevance of the use of CFD models in this type of problem.

This statement can also be demonstrated by analyzing the values of the average velocity gradient value (G_{av}). This is a parameter generally used in sanitary design and can be estimated based on ϵ and νZ (kinematic viscosity of the fluid), as follows:$G_{av} = (\epsilon/\nu)^{1/2}$. In the sections A-A and B-B, G_{av} values are in the order of 20–80 Hz, which is acceptable for flocculation to occur (Tambo & François 1991). However, in section C-C the values G_{av} are significantly higher than in section A-A. Thus, turbulence could cause the breakage of the flocs generated in the mixing chamber. Previous studies show that the size of the flocs formed in the flocculation process (with G_{av} equal to 50 Hz) decays to a minimum size when the particles are subjected to G_{av} values of 100, 300 and 500 Hz after 1 minute. The latter values are similar to those found in the B-B and C-C sections, and in gates 3 and 4 of the treatment plant. Finally, the presence of particles of smaller size and weight generates low efficiency of the sedimentation tanks with floc volumes extraction below those provided in the design.

Figure 6 shows a good agreement by comparing the observed and simulated longitudinal flow velocity field for the in-situ measurement 6 (see Table 1), along section G-G.

It can be observed that the numerical model correctly represents the observed zones of flow stagnation (flow velocities close to zero) in the region between Y-axis 0 (wall of the transverse-channel) and 0.5 m. Something similar occurs downstream of the central pile of the gateway (Y-axis 9.5 m).

Transverse-channel data were recorded with the ADCP during the in-situ measurement 6 in section H-H (see Figure 2(b)). Figure 7 compares the flow velocity magnitude for the transverse-channel. Similar patterns are observed in both measured and simulated areas of stagnant flow and velocity magnitude. Note that the transverse-channel has a

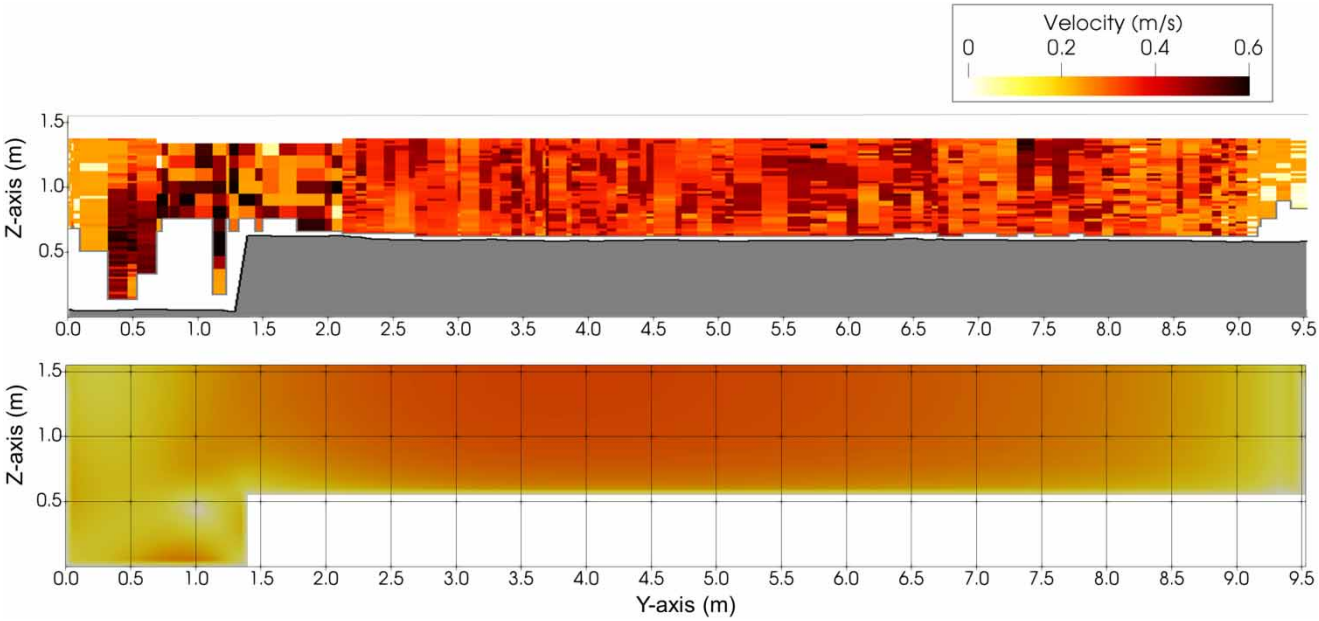

Figure 6 | Observed (top frame) and simulated (bottom frame) values of the mean longitudinal flow velocity component along section G-G (in-situ measurement 6). The zero in the Y-axis corresponds to the wall of the transverse-channel.

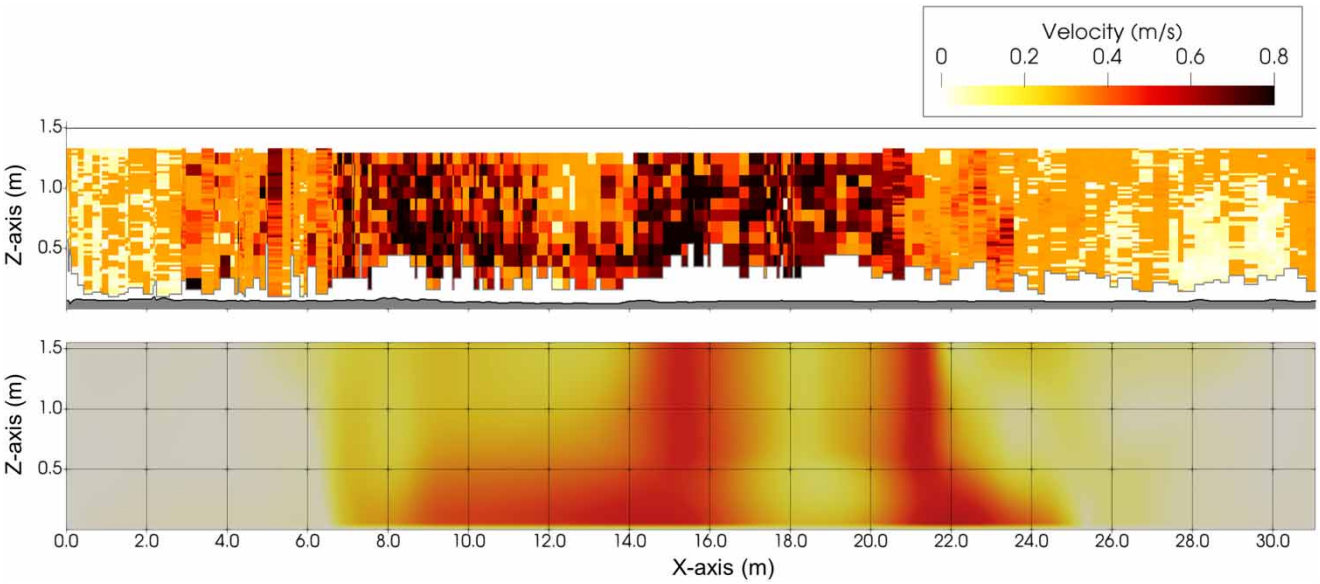

Figure 7 | Observed (top frame) and simulated (bottom frame) distribution of the flow velocity magnitudes for the transverse-channel.

large region of stagnant flow (flow velocity magnitude close to zero), 6 m to the left side (X-axis 6 m in Figure 7) and 5 m to the right side (X-axis 26 m in Figure 7).

As a summary of the numerical model validation it can be stated that: (a) the experimental data collected in the flume were successfully used as boundary conditions for validating the numerical model; (b) the open-source toolbox OpenFOAM® adapts to the problem in an appropriate way and indicates the relevance of using CFD models in this type of study case; (c) the use of a rigid lid at the free surface was allowed to solve the problem without requiring the use of a two phase flow simulation scheme with a consequent reduction in complexity in the numerical model; (d) the numerical model accurately

reproduces the average values of flow velocities (characterizing flow stagnation and acceleration zones), and the largest differences were found in the recirculation zones where a non-stationary phenomenon occurs; (e) the model accurately simulates the spatial evolution of k.

Analysis and optimization of water treatment plant operation

In this case, the smaller largest ϵ observed in sections B-B and C-C indicates that the flocs formed in the mechanical agitators located upstream in the treatment plant would break in these sections.

Once the numerical model was validated, it was used to simulate two operating conditions of the water treatment plant and to characterize the flow stagnation and acceleration zones as well as the spatial evolution of k and ϵ.

Firstly, the case where the treatment plant operates with 3 settling tanks was numerically modeled; that is, while one settling tank is under maintenance (tank cleaning, for example). The results were compared with the results in normal operating conditions (4 settling tanks working).

Figures 8 shows values of the velocity field for the hydraulic conditions obtained in in-situ measurement 1 in the study area, when the treatment plant operates with three sedimentation tanks: Figure 8(a)–8(c) for settling tank 1, 2 or 3 under maintenance, respectively. These figures show an increase in the velocity value in the opposite branch of the transverse-channel where the settling tank is out of service, owing to a redistribution of the discharge among the three operating tanks. Also, the maximum k

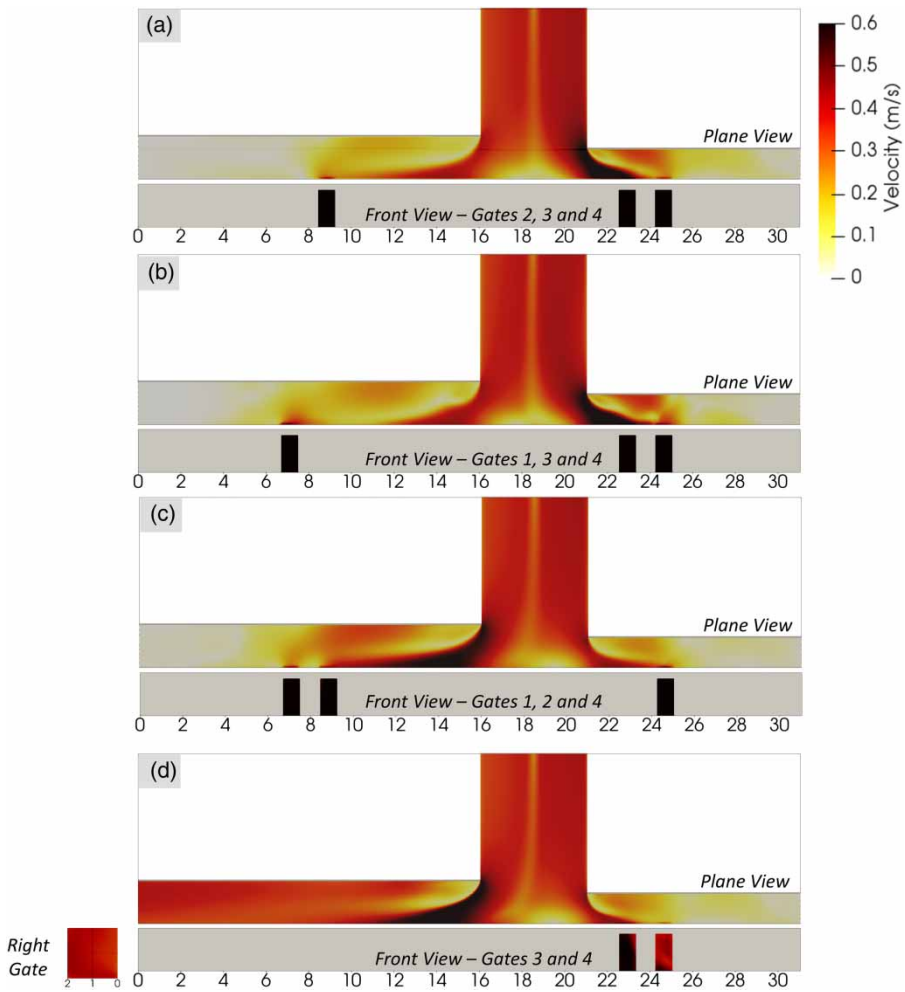

Figure 8 | Plane view: mean velocity magnitude at z = 1.55 m. Front view: mean velocity magnitude at gates. Numerical model results when the treatment plant operates with 3 settling tanks. (a) Settling tank 1, (b) settling tank 2 and (c) settling tank 3 under maintenance. (d) Numerical model results when the treatment plant operates in an emergency situation: only settling tanks 3 and 4 are in use.

values are in the order of 600 cm^2/s^2 in the transverse-channel and the order of 1,000 cm^2/s^2 at the gates. These values are larger than the recommended maximum values for normal operating conditions (four settling tanks, see Table 3). These results indicate that it would be recommended to perform maintenance and cleaning tasks firstly on tanks 1 and 2, and then on tanks 3 and 4.

Secondly, the treatment plant was modeled in an emergency situation; that is, only settling tanks 3 and 4 are in use, while a gate at the end of the right side of the transverse-channel is opened and settling tanks 1 and 2 were bypassed. The outflow at the right gate is then mixed with a coagulant and goes directly to the filtering process.

Figure 8(d) shows the flow velocity field resulting from the simulation of this operational condition. Velocity magnitudes in gates 3 and 4 are similar to those for the normal operating conditions and the k values indicate that flocs reach their smaller size on the gates of sedimentation tanks 3 and 4.

The experimental and numerical characterization presented up to here indicates that geometric modifications are needed in the transition zone from the flume to the transverse-channel and in the gates, since in these zones the flocs break into smaller particles and, therefore, decrease the settling tanks' efficiency.

It is important to highlight that the validated CFD model is now available for the Aguas Cordobesas SA Company to apply in future hydraulic design optimization studies for the water treatment plant 'Los Molinos'.

CONCLUSIONS

In this work, experimental and numerical characterizations of the incoming flow to the clarification component of the water treatment plant 'Los Molinos', Córdoba, Argentina, has been presented.

The experimental characterization has been performed using advanced flow velocity measurement techniques; that is, an ADV and an ADCP. Both these techniques provide valuable information not only for turbulent flow characterization, but also for the definition of boundary conditions and thus helping the validation of the numerical model used.

The results of the experimental work show a strong three-dimensional flow with high turbulence intensity in sections B-B and C-C, and a strong flow separation zone that affects 50% of the cross-sectional width. Turbulent kinetic energy values in that zone are one order of magnitude larger than those observed in the upstream flume cross-section, and thus the Kolmogorov length scale reaches its minimum value.

At this point the flocs break into smaller particles, inducing a lower efficiency in the sedimentation tanks, with floc volume extractions below those provided in the design manuals.

A numerical vertical Reynolds-averaged Navier-Stokes (RANS) equations model was employed, using a k-ϵ standard turbulence closure. This numerical model accurately reproduces the mean flow velocity values (characterizing flow stagnation and acceleration zones), the spatial evolution of turbulent kinetic energy and the dissipation rate. This indicates that a RANS k-ϵ model (with sufficient mesh resolution) is a valid engineering tool in order to obtain turbulence characteristic parameters such as k and ϵ, directly related to the floc size. The largest differences between experimental observations and numerical results were found in the recirculation zones where non-stationary phenomena occur.

It should be stated that the use of a rigid lid at the top surface allowed solving of the problem without requiring the use of a two-phase flow simulation scheme; that is, with a consequent reduction in numerical model complexity

Also, the open-source toolbox OpenFOAM® was shown to accurately represent the observations and so indicates the relevance of the use of CFD models in this type of study case.

Further, the validated model was used to simulate two different operating conditions: (a) the treatment plant operating with only 3 settling tanks while one was under maintenance (tank cleaning, for example); and (b) the treatment plant operating in an emergency situation with only two settling tanks (settling tanks 1 and 2 were bypassed).

Both the experimental and the numerical characterizations presented indicate that geometric modifications are needed in the transition zone from the flume to the transverse-channel and in the gates, because in these zones the flocs break into smaller particles and therefore decrease the settling tanks' efficiency.

Finally, the validated CFD model is available for Aguas Cordobesas SA company to be applied in future studies for hydraulic design optimization in 'Los Molinos' water treatment plant.

FUTURE RESEARCH

We strengthen the need to incorporate a sediment transport model and a floc breakage model in order to improve and to

complement the characterization of the problems observed in the areas upstream of the clarification components.

ACKNOWLEDGEMENTS

The authors would like to thank the manager staff as well as the professionals and technicians from Aguas Cordobesas SA responsible for operating the water treatment plant 'Los Molinos', near the town of Bower, province of Córdoba, Argentina. Authors would also like to thank the Secretary of Science and Technology of the National University of Cordoba (SECyT-UNC) and the National Council for Scientific and Technological Research (CONICET) for funding this project.

REFERENCES

Adams Jr., C. E., Aulenbach, D. B., Bollyky, L. J., Boyd, J. L., Buchanan, R. D., Burns, D. E., Canter, L. W., Crits, G. J., Dahlstrom, D., Daniels, S. L., Dittman, F. W., Echelberger Jr., W. F., Gantz, R. G., Gilde Jr., L. C., Goodman, B. L., Harfouche, N., Holbrook, R. D., Hong, S. N., Huibers, D. T. A., Keith Jr., F. W., Lee, M. K., Lipták, B. G., Lipták, J., Liu, D. H. F., McGarvey, F. X., Myron Jr., T. J., Nguyen, V. T., Rabosky, J. G., Reuter, L. H., Rico-Ortega, B., Santhanam, C. J., Savage, E. S., Sebastian, F. P., Shell, G. L., Shieh, W. K., Snell, J. R., Stavenger, P. L. & Switzenbaum, M. S. (1999) *Wastewater Treatment, Environmental Engineers' Handbook*. CRC Press LLC, Boca Raton, FL, pp. 7.17

De Clercq, B., Kinnear, D. J. & Vanrolleghem, P. A. 2002 Hydraulic characterization of a wastewater treatment clarifier by an acoustic Doppler current profiler. In: *Advances in Fluid Mechanics IV* (M. Rahman, R. Verhoeven & C. A. Brebbia, eds). WIT Press, Southampton, UK, pp. 451–462.

Ducoste, J. J., Clark, M. & Weetman, R. J. 1997 Turbulence in flocculators: the effects of tank size and impeller type. *AIChE Journal* **43** (2), 328.

Garcia, C. M. & Garcia, M. 2006 Characterization of flow turbulence in large-scale bubble-plume experiments. *Experiment in Fluids* **41**, 91–101.

García, C. M. & Herrero, H. 2009 Metodología Experimental Para Caracterizar Flujos Turbulentos Con Velocímetros Acústicos Doppler. In: *I Simposio sobre Métodos Experimentales en Hidráulica, Carlos Paz, Córdoba, Argentina*.

García, C., Jackson, P. & Garcia, M. 2006 Confidence intervals in the determination of turbulence parameters. *Experiment in Fluids* **40**, 514–522.

Goula, A. M., Kostoglou, M., Karapantsios, T. D. & Zouboulis, A. I. 2008 A CFD methodology for the design of sedimentation tanks in potable water treatment case study: the influence of a feed flow control baffle. *Chemical Engineering Journal* **140**, 110–121.

Huggins, D. L., Piedrahita, R. H. & Rumsey, T. 2004 Analysis of sediment transport modeling using computational fluid dynamics (CFD) for aquaculture raceways. *Aquacultural Engineering* **31**, 277–293.

Kiss, K. & Patziger, M. 2013 Novel measurements in primary settling tanks of large municipal wastewater treatment plants. *YBL Journal of Built Environment* **1** (1), 6–18.

Launder, B. E. & Sharma, B. I. 1974 Application of the energy dissipation model of turbulence to the calculation of flow near a spinning disc. *Letters in Heat and Mass Transfer* **1** (2), 131–138.

Launder, B. E. & Spalding, D. B. 1972 *Lectures in Mathematical Models of Turbulence*. Academic Press, New York, NY.

Launder, B. E. & Spalding, D. B. 1974 The numerical computation of turbulent flows. *Computer Methods in Applied Mechanics and Engineering* **3** (2), 269–289.

Laurent, J., Samstag, R. W., Ducoste, J. M., Griborio, A., Nopens, I., Batstone, D. J., Wicks, J. D., Saubers, S. & Potier, O. 2014 A protocol for the use of computational fluid dynamics as a supportive tool for wastewater treatment plant modeling. *Water Science and Technology* **70** (10), 1575–1584.

OpenCFD Available from: http://www.opencfd.co.uk/openfoam/.

OpenFOAM Wiki The SIMPLE algorithm in OpenFOAM. Last visited: 2012-09-27. Mar. 2010. Available from: http://openfoamwiki.net/index.php/The_SIMPLE_algorithm_in_OpenFOAM.

Patziger, M. & Kiss, K. 2015 Analysis suspended solids transport processes in primary settling tanks. *Water Science and Technology* **72** (1), 1–9.

Patziger, M., Günthert, F. W., Jardin, N., Kainz, H. & Londong, J. 2016 On the design and operation of primary settling tanks in state of the art wastewater treatment and water resources recovery. *Water Science and Technology* **74** (9), 2060–2067.

Robertson, E., Choudhury, V., Bhushan, S. & Walters, D. K. 2015 Validation of OpenFOAM numerical methods and turbulence models for incompressible bluff body flows. *Computers & Fluids* **123**, 122–145.

Samstag, R. W., Ducoste, J. J., Griborio, A., Nopens, I., Batstone, D. J., Wicks, J. D., Saunders, S., Wicklein, E. A., Kenny, G. & Laurent, J. 2016 CFD for wastewater treatment: an overview. *Water Science and Technology* **74** (3), 549–563.

Shahrokhi, M., Rostami, F., Md Said, M. A. & Syafalni, S. 2011 Numerical investigation of baffle effect on the flow in a rectangular primary sedimentation tank. *World Academy of Science, Engineering and Technology. International Journal of Environmental, Chemical, Ecological, Geological and Geophysical Engineering* **5** (10), 571–576.

Takano, Y. & Moonen, P. 2013 On the influence of roof shape on flow and dispersion in an urban street canyon. *Journal of Wind Engineering and Industrial Aerodynamics* **123**, 107–120.

Tambo, N. & François, R. 1991 Mixing, Breakup, and floc characteristics. In: *Mixing in Coagulation and Flocculation* (A. Amirtharajah, M. Clark & R. Trussell, eds). AWWA RF Press, Denver, CO. Cap. 5, pp. 256–281.

Vanrolleghem, P. A., De Clercq, B., De Clercq, J., Devisscher, M., Kinnear, D. J. & Nopens, I. 2006 New measurement

techniques for secondary settlers: a review. *Water Science and Technology* **53**, 419–429.

Versteeg, H. K. & Malalasekera, W. 2007 *An Introduction to Computational Fluid Dynamics. The Finite Volume Method*, 2nd edn. Pearson Education Limited, London, UK.

Wei, W., Bai, Y. & Liu, Y. 2016 Optimization of submerged depth of surface aerators for a carrousel oxidation ditch based on large eddy simulation with Smagorinsky model. *Water Science and Technology* **73** (7), 1608–1618.

Wicklein, E., Batstone, D. J., Ducoste, J., Laurent, J., Griborio, A., Wicks, J., Saunders, S., Samstag, R., Potier, O. & Nopens, I. 2016 Good modelling practice in applying computational fluid dynamics for WWTP modelling. *Water Science and Technology* **73** (5), 969–982.

Zhang, D. 2014 *Optimize Sedimentation Tank and Lab Flocculation Unit by CFD*. Department of Mathematical Science and Technology (IMT), Norwegian University, Trondheim, Ålesund, Gjøvik, Norway.

First received 12 August 2019; accepted in revised form 8 January 2020. Available online 21 January 2020